Cholinergic Differentiation of Human Neuroblastoma SH-SY5Y Cell Line and Its Potential Use as an In vitro Model for Alzheimer's Disease Studies

Liana M. de Medeiros [1,2,3] · Marco A. De Bastiani [1,2,3] · Eduardo P. Rico [4] · Patrícia Schonhofen [1,2,3] ·
Bianca Pfaffenseller [1,2,5] · Bianca Wollenhaupt-Aguiar [1,2,5] · Lucas Grun [3,6] · Florência Barbé-Tuana [3,6] ·
Eduardo R. Zimmer [3,7,8] · Mauro A. A. Castro [9] · Richard B. Parsons [10] · Fábio Klamt [1,2,3]

Abstract

Cholinergic transmission is critical to high-order brain functions such as memory, learning, and attention. Alzheimer's disease (AD) is characterized by cognitive decline associated with a specific degeneration of cholinergic neurons. No effective treatment to prevent or reverse the symptoms is known. Part of this might be due to the lack of in vitro models that effectively mimic the relevant features of AD. Here, we describe the characterization of an AD in vitro model using the SH-SY5Y cell line. Exponentially growing cells were maintained in DMEM/F12 medium and differentiation was triggered by the combination of retinoic acid (RA) and BDNF. Both acetylcholinesterase (AChE) and choline acetyltransferase (ChAT) enzymatic activities and immunocontent were determined. For mimicking tau and amyloid-β pathology, RA + BDNF-differentiated cells were challenged with okadaic acid (OA) or soluble oligomers of amyloid-β (AβOs) and neurotoxicity was evaluated. RA + BDNF-induced differentiation resulted in remarkable neuronal morphology alterations characterized by increased neurite density. Enhanced expression and enzymatic activities of cholinergic markers were observed compared to RA-differentiation only. Combination of sublethal doses of AβOs and OA resulted in decreased neurite densities, an in vitro marker of synaptopathy. Challenging RA + BDNF-differentiated SH-SY5Y cells with the combination of sublethal doses of OA and AβO, without causing considerable decrease of cell viability, provides an in vitro model which mimics the early-stage pathophysiology of cholinergic neurons affected by AD.

Keywords Retinoic acid · BDNF · Cholinergic neurons · SH-SY5Y

Abbreviations

AD	Alzheimer's disease
DMEM	Dulbecco's Modified Eagle Medium
FBS	Fetal bovine serum
RA	Retinoic acid
BDNF	Brain-derived neurotrophic factor
AChE	Acetylcholinesterase
ChAT	Choline acetyltransferase

✉ Fábio Klamt
fabio.klamt@ufrgs.br

1 Laboratory of Cellular Biochemistry, Department of Biochemistry, ICBS/UFRGS, 2600 Ramiro Barcelos St, Porto Alegre, RS 90035-003, Brazil

2 National Institutes of Science and Technology–Translational Medicine (INCT-TM), Porto Alegre, Brazil

3 Post-Graduate Program in Biochemistry, Department of Biochemistry, ICBS/UFRGS, Porto Alegre, RS 90035-003, Brazil

4 Programa de Pós-Graduação em Ciências da Saúde, Unidade Acadêmica de Ciências da Saúde, Universidade do Extremo Sul Catarinense (UNESC), Criciúma, SC 88806-000, Brazil

5 Department of Psychiatry and Behavioral Neurosciences, McMaster University, Hamilton, ON, Canada

6 Laboratory of Molecular Biology and Bioinformatics, Department of Biochemistry, ICBS/UFRGS, Porto Alegre, RS 90035-003, Brazil

7 Brain Institute of Rio Grande do Sul (BraIns), Pontifical Catholic University of Rio Grande do Sul (PUCRS), Porto Alegre, RS, Brazil

8 Department of Pharmacology, ICBS/UFRGS, Porto Alegre, RS, Brazil

9 Bioinformatics and Systems Biology Laboratory, Polytechnic Center, Federal University of Paraná (UFPR), Curitiba, PR 81520-260, Brazil

10 School of Cancer and Pharmaceutical Sciences, King's College London, 150 Stamford Street, London SE1 9NH, UK

AβOs	Amyloid-β oligomers
AO	Okadaic acid
MTT	3-(4,5-Dimethylthiazol-2il)-2,5-diphenyltetrazolium bromide
DAT	Dopamine transporter
Aβ	Amyloid-β
BFC	Basal forebrain complex
APP	Amyloid precursor protein
ACh	Acetylcholine
CDK5	Cyclin-dependent kinase

Introduction

Alzheimer's disease (AD) is a disorder clinically characterized by progressive cognitive decline, including disruptions in memory and reasoning, leading to a state of dementia [1, 2]. This cognitive impairment is correlated with the dysfunction and degeneration of cholinergic neurons located in the basal forebrain complex (BFC), which is an early pathological event of the disease [3, 4]. Histologically, AD is characterized by two main pathological hallmarks: neurofibrillary tangles and extracellular deposits of Amyloid-β (Aβ) [5]. Neurofibrillary tangles are formed by unfolded protein aggregates constituted mainly of hyperphosphorylated tau protein [6]. The extracellular deposits consist of Aβ peptides which are products of an irregular cleavage of amyloid precursor protein (APP) [7, 8]. In AD, APP is abnormally cleaved, forming Aβ peptides that produce amyloid deposits known as amyloid plaques [8, 9]. Aβ is a 40 ($Aβ_{1-40}$) or 42 ($Aβ_{1-42}$) amino acids peptide, of which $Aβ_{1-42}$ is the most toxic and faster-aggregating form [10]. However, the molecular mechanisms underlying the formation of toxic aggregates have not been fully elucidated. This might be due in part to the lack of suitable in vitro models resembling mature human cholinergic neurons [11, 12]. Most common in vitro models within AD research include cell lines that lack proper neurite structures and many of the features that define neurons, such as mature neuronal markers [12, 13]. Also, the use of primary rodent neurons derived from embryonic central nervous system tissue is limited by the fact that they do not express the human proteins most closely associated with neurodegenerative diseases [14]. Still, human stem cells offer high risks of mutations and, as well as 3D human neural cell culture, are time consuming, highly expensive [15], and are thus not suitable for high-throughput studies. However, differentiated neuronal-*like* cell lines can be used to overcome this limitation. The human neuroblastoma cell line SH-SY5Y is frequently used as an in vitro model for neurodegenerative disease studies. SH-SY5Y cells are derived from the sympathetic nervous system and considered to be derived from a neuronal lineage in its immature stage. This cell line is characterized by continuously proliferation, expression of immature neuronal proteins, and low abundance of

neuronal markers [16, 17]. Many lines of evidence have indicated that, according to the protocol used, these cells are able to differentiate and acquire mature neuron-*like* features [18–21]. Following neuronal differentiation, SH-SY5Y neuroblastoma cells unfold a number of morphological and biochemical events, including a decrease in proliferation rate, formation and extension of neurites, and expression of mature neuronal markers, thus becoming phenotypically closer to primary neurons. Most importantly, SH-SY5Y cells express human proteins [17, 22].

The most commonly known differentiation protocol implemented is through addition of retinoic acid (RA) to the cell culture medium [17]. The reduction of media serum content to 1% plus supplementation with 10 μM RA results not only in neurite outgrowth, but also increase in expression of neuronal markers, such as tyrosine hydroxylase (TH), neuron-specific enolase (NSE), neuronal nuclei protein (NeuN), and the dopamine transporter (DAT) [21, 23]. A number of alternative differentiation methods have also been described. For instance, treatments with neurotrophins such as nerve growth factor (NGF) and brain-derived neurotrophic factor (BDNF) have been shown to induce the differentiation of SH-SY5Y cells [14, 18]. RA differentiation induces the expression of TrkB receptor, which turn cells responsive to BDNF [24, 25].

It has also been described that growth factors play an important role in protection and maintenance of cholinergic neurons [26, 27]. Cholinergic neurons from BFC are involved in learning, memory, and sleep cycle [28–30] and display a selective vulnerability in AD [27, 31]. Also, a number of studies have shown that BDNF is essential to cholinergic differentiation in brain development [26, 32]. Hence, it is of crucial importance to also explore this hallmark in AD models. Although the combination of BDNF and RA for differentiating cells has been already described [11, 19], its role in a cholinergic neuronal phenotype in SH-SY5Y cells is yet to be exploited. Here, we present a method for the differentiation of SH-SY5Y cells into a cholinergic phenotype using a combination of RA and BDNF, with further challenges with okadaic acid and soluble Aβ oligomers which is suitable for AD-based studies.

Materials and Methods

Cell Culture and Differentiation

Exponentially growing human neuroblastoma cell line SH-SY5Y, obtained from ATCC (Manassas, VA, USA), was maintained at 37 °C in a humidified atmosphere of 5% of CO_2. Cells were grown in a mixture of 1:1 of Ham's F12 and Dulbecco Modified Eagle Medium (DMEM, Gibco®/Invitrogen, Sao Paulo, Brazil) supplemented with 10% heat-inactivated fetal bovine serum (FBS) (Cripion®, Sao Paulo,

Brazil) and antibiotic/antimycotic (Gibco® 15240-062). Cell medium were replaced every 3 days and cells were sub-cultured once they reached 80% confluence. Only attached cells were maintained and floating cells were discarded. To evaluate the effects of BDNF, we designed two distinct differentiation protocols. A general description is depicted in Fig. 1. Neuronal differentiation was induced by treatment with RA (Enzo® Life Sciences, Lörrach, Germany) and BDNF (Human Recombinant, Prospec®, NJ, USA). After 24 h of plating, differentiation was initiated by lowering FBS in

culture medium to 1% and supplementing with 10 μM RA for 7 days. This treatment was replaced every 3 days to replenish RA in the culture media. Same treatment was performed with the addition of 50 ng/mL BDNF on the fourth day of differentiation with RA. RA stock solutions were prepared in absolute ethanol and the concentration determined using E^M (351 nm) = 45000 [33]. BDNF stock solution at a concentration of 100 μg/mL was prepared by dissolving it in a solution of 0.1% bovine serum albumin (BSA) according to the manufacturer.
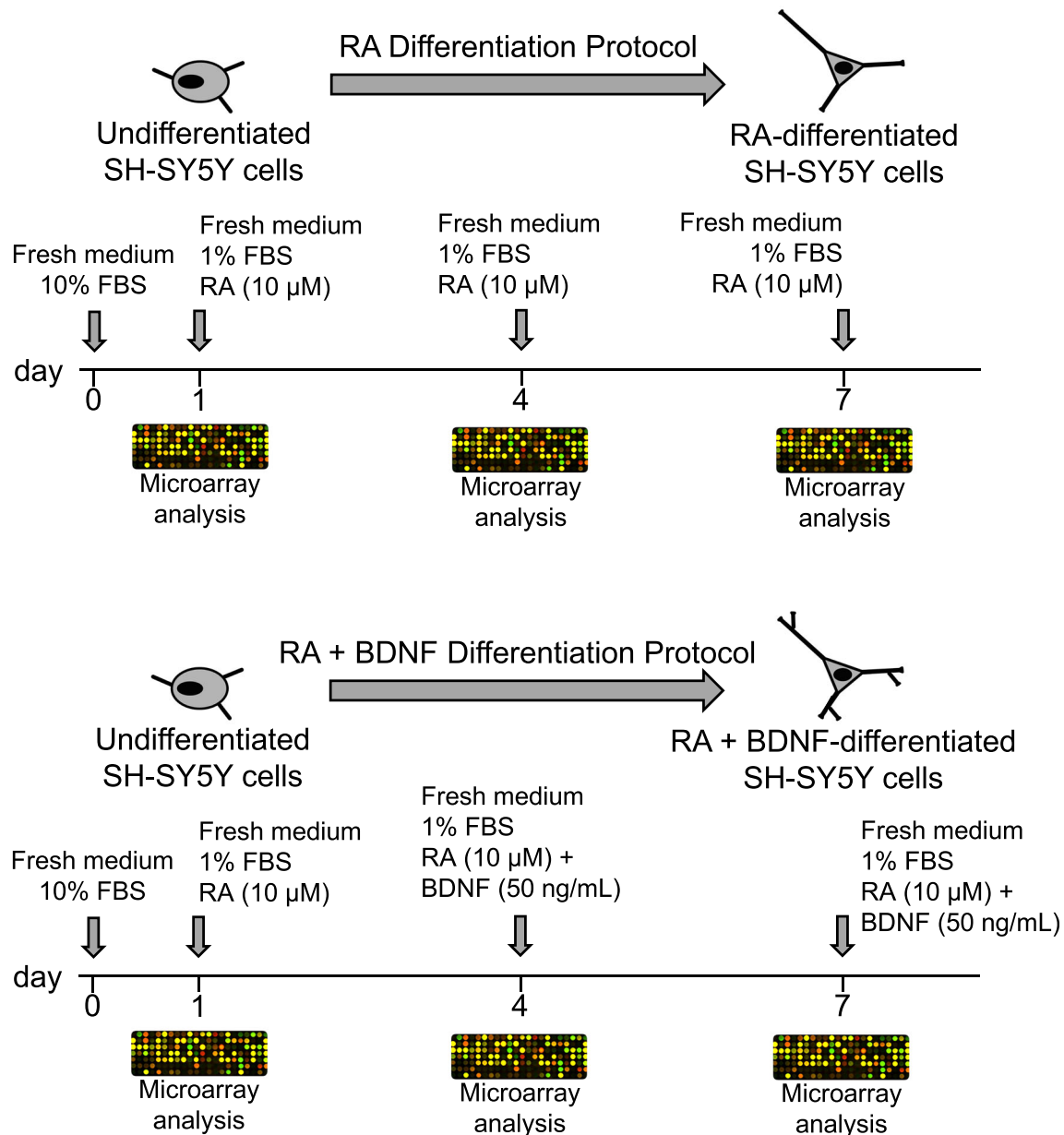

Fig. 1 Differentiation protocols. Proliferative SH-SY5Y cells are seeded and cultured in medium supplemented with 10% FBS for 24 h for complete adhesion. Then, biochemical and microarray analyses were performed. For RA treatment (upper panel), differentiation is induced after cell adhesion with the reduction of FBS to 1% and the addition of 10 μM of AR, which is considered the first day. Lower panel shows that 50 ng/mL BDNF is added on the fourth day combined with RA replenishment. Microarray analyses were also performed on day 4 and 7

RNA Isolation and Microarray Assay

To explore the effects of BDNF on genetic networks, total RNA samples were extracted using TRIzol™ reagent (Thermo Fisher Scientific®, Waltham, MA, USA) following purification (Qiagen RNeasy Mini Kit #74104 and #79254—Free RNase DNase set, Hilden, Germany). Microarray was performed using GeneChip® PrimeView™ Human Gene Expression Array (Affymetrix™). Samples were collected at day 0 (undifferentiated cells), day 4 (RA-differentiated cells), and day 7 (RA- and RA + BDNF-differentiated cells) as shown in Fig. 1. Raw data were deposited in the GEO repository (GEOID: GSE71817).

Raw microarray CEL files were analyzed using the R/Bioconductor pipeline. The data was normalized by Robust Multi-Array Average (RMA) in the AFFY package [34], log (base 2) transformed, and batch-corrected with ComBat in the SVA package [35].

Enrichment Analysis and Expression Values

Three gene sets were analyzed: Alzheimer's disease network, cholinergic synapse, and neurotrophin signaling network (extracted from the *Kyoto Encyclopedia of Genes and Genomes* (KEGG) platform—KEGG Pathway Database, 2017: http://www.genome.jp/kegg/pathway.html). Gene set enrichment analysis (GSEA) considered experiments with genome-wide expression profiles from two classes of samples (e.g., 7-day-RA + BDNF-differentiated cells vs.7-day-RA-differentiated cells, and RA + BDNF-differentiated cells vs. undifferentiated cells). Genes were ranked based on the correlation between their expression and the class association. Given a prior defined network (e.g., cholinergic synapse), GSEA determines if the members of these sets of genes are randomly distributed or primarily found at the top or bottom of the ranking [36].

Morphological Analysis

To assess changes in morphological parameters between RA-differentiated and RA + BDNF-differentiated cells, we evaluated neuronal morphology and neurite densities. Firstly, neuronal morphology was assessed through scanning electron microscopy (SEM). Cells were seeded onto glass coverslips in 24-well plates at a density of 6×10^4 cells per well. Cells were fixed by immersion in 25% glutaraldehyde for 1 week. Next, cells were washed in 0.2 M phosphate buffer. For dehydration, sequential immersions in acetone 30% to 100% were performed. Drying was carried out in a Critical Point Dryer (Balzers CPD030). Metallization process used gold as metal target (Sputter Coater, Balzers SCD050).

Fig. 2 **a** Gene enrichment analysis was used to identify genes in ▶ neurotrophic signaling network which expression would be affected by the RA treatment on day 1 and 4. Morphometric Analysis: **b** *Left panel:* representative segmented immunofluorescence images of proliferative SH-SY5Y cells, differentiated for 7 days with RA and co-treated with BDNF. Fluorescent labeling in green indicates βIII-tubulin (neuron-specific) evidencing neurites, superimposed on nuclear labeling with Hoechst 33342 (200X). *Right panel:* Histograms representing automated neurite quantification of segmented images generated by the software AutoQuant Neurite®. The statistics test used was Tukey's ($p < .001$). **c** Representative images of scanning electronic microscopy of cells submitted to the three differentiation protocols. Ten microscopic fields (× 200 magnification) were selected from three independent experiments ($n = 3$)

Neurite Density

Neurite densities of RA + BDNF-differentiated cells, OA, Aβ, or combined treatments were evaluated using immunofluorescence. Cells were washed with phosphate buffered saline (PBS), fixed with 1:1 methanol:acetone (20% *v/v*) for 20 min at room temperature (RT), and permeabilized with 0.2% Triton X-100-supplemented PBS. Nonspecific binding was blocked with 1% BSA for 1 h at RT. After PBS washes, cells were incubated with conjugated anti-β-tubulin III (Alexa Fluor®488, 1:50, Abcam) for 2 h at RT followed by nuclear dye Hoechst 33342 (Molecular Probes® Life Technologies) incubation for 15 min (1 μg/μL). Ten microscopic fields (× 200 magnification) were selected randomly from each of three independent experiments ($n = 3$). Images were captured with NIS elements software, using an Olympus IX70 inverted microscope. Neurite density was assessed using the AutoQuant Neurite software (implemented in *R* language) and expressed as arbitrary units (A.U.).

RNA Isolation and Real-Time qPCR Assay

Gene expression analysis was performed using gene-specific primers designed with IDT Design Software (Integrated DNA Technologies Inc., CA, USA). Total RNA was isolated from SH-SY5Y cells using TRIzol™ Reagent (Thermo Fisher Scientific®, Waltham, MA, USA). Samples were transcribed into cDNA using random nonamers (Sigma-Aldrich®, St. Louis, MO, USA) and M-MLV Reverse Transcriptase (Sigma-Aldrich®). Real-time PCR reactions were carried out in Step One Plus real-time cycler (Applied-Biosystem®, NY, USA) using Taq polymerase (Sigma-Aldrich®) and SYBR green. Gene expression was quantified by the comparative cycle threshold method ($\Delta\Delta$CT) and normalized using the housekeeping gene *RACK1*. Melting curves were used to monitor unspecific amplification products. The amplification reaction consisted of a hold of 10 min at 95 °C and 40 cycles with subsequent recording of primer melting curves. The primers sequences for amplification of the target genes were CDK5: HsCDK5Fwd: CGAGAAACTGGAAAAGATTG
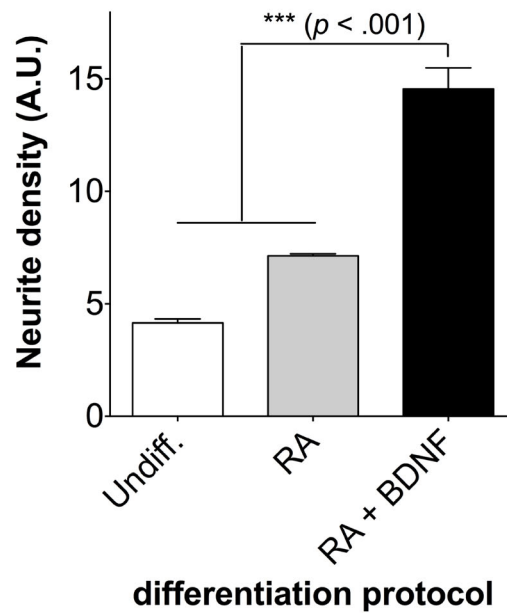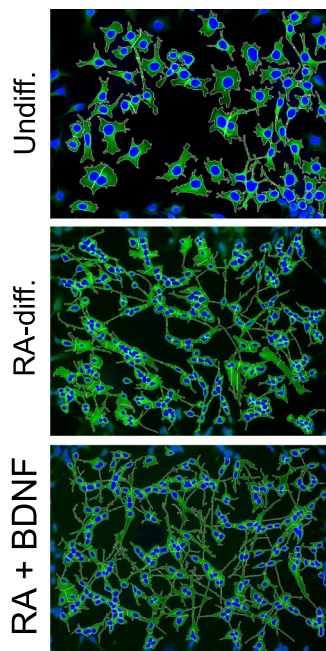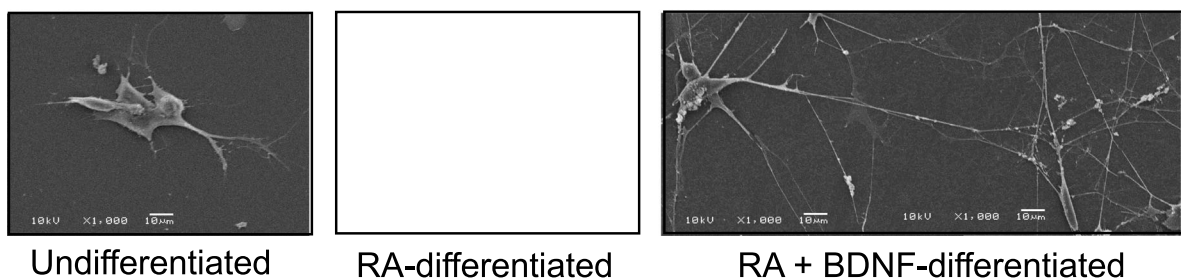
Neurotrophin Signaling Network

a)

Morphometric Analysis

b)

c)

Undifferentiated   RA-differentiated   RA + BDNF-differentiated
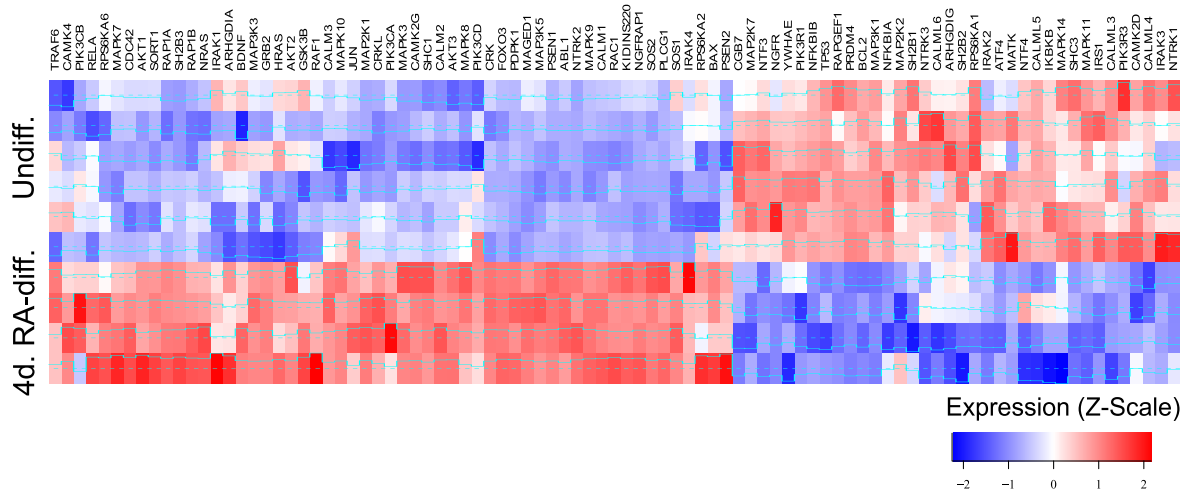
GG, and HsCDK5Rev: TTTCAGAGCCACGATCTCATG.
PSEN1: HsPSEN1Fwd: GGTGAATATGGCAGAAGGAG
AC, and HsPSEN1Rev: AGGGCTTCCCATTCCTCACTG.
SCL18A: HsSCL18Fwd: GTCCTCGGAAGAGCATCG,
and HsSCL18Rev: CACACGATAACAAGCACCAG.

Cholinergic Enzyme Activities

AChE (EC 3.1.1.7) enzymatic activity was determined by the
colorimetric assay described by Ellman [37]. Cells were
washed twice in PBS (pH 7.4) and total protein was extract
with lysis buffer (20 mM HEPES, 150 mM NaCl and 1% NP-
40) with the addition of protease and phosphatase inhibitors
(Roche® Basel, Switzerland). Cell lysates were incubated for
5 min in 10 mM 5,5′-dithiobis (2-nitrobenzoic acid) (DTNB)
(Sigma®). Acetylthiocholine (8 mM, Sigma®) was added to
this mixture and absorbance was measured at 412 nm for
10 min. Results were expressed as μmol/min/mg of protein.
The activity of the enzyme choline acetyltransferase (ChAT)
(E.C. 2.3.1.6) was determined according to Chao & Wolfgram
[38] with some minor modifications. Samples were incubated
with reaction buffer (PBS pH 7.2, 6.2 mM acetylcoenzyme A,
1.0 M choline chloride, 0.76 mM neostigmine sulfate, 3 M
NaCl and 1.1 mM EDTA). To initiate the reaction, 1 mM 4,4′-
dithiodipyridine (4- PDS) was added and the absorbance was
measured for 90 min at 324 nm using a SpectraMax®
Microplate Reader (Molecular Devices®). Results were
expressed in nmol/min/mg of protein based on the molar ex-
tinction coefficient of 1.98×10^4.

Western Blot

For western blot analysis, 3×10^6 cells were seeded into
75 cm² flasks. After 24 h plating or after differentiation treat-
ment, cells were washed with PBS and suspended in lysis
buffer (1% (w/v) SDS, 10 mM TRIS, 1 mM EDTA) supple-
mented with protease and phosphatase inhibitors (Roche®
Basel, Switzerland). Total protein extracts were separated by
sodium dodecyl sulfate-polyacrylamide gel electrophoresis
(SDS-PAGE) and then transferred onto a polyvinylidene
difluoride (PVDF) membrane. Thereafter, nonspecific binding
was blocked with 5% of BSA in Tris-buffered saline 0.1%
Tween 20 (TBST) for 1 h at RT. Membranes were then incu-
bated overnight at 4 °C with mouse anti-DAT antibody
(1:1000, Santa Cruz® Biotechnology, Dallas, Texas, USA),
rabbit anti-ChAT (1:1000, Abcam), rabbit anti-Tau (1:500,
Abcam), or mouse anti-phospho-Tau Ser$_{202-199}$ (Invitrogen,
Waltham, Massachusetts). After washing, the membrane was
incubated with peroxidase-conjugated secondary antibodies
(1:5000, Dako®, Glostrup, Denmark) for 2 h at RT. Bands
were visualized with Super Signal West Pico
Chemiluminescent Substrate (PIERCE®, Rockford, Il,
USA). For the loading control, membranes were subsequently

stripped and reprobed with rabbit anti-β-actin (1:5000, Santa
Cruz Biotechnology, Inc.) followed by goat anti-rabbit perox-
idase-conjugated secondary antibody (1:5000, Dako®).
Protein content was measured using Lowry assay (Bradford,
1976).

Amyloid-β Oligomerization Protocol

Soluble AβOs were prepared according to Klein (2002) [39].
Human Aβ peptides (Abcam®) were diluted in 1,1,1,3,3,3-
hexafluoro-2-propanol (HFIP) (Sigma®) at a concentration of
1 mM and incubated at RT for 1 h. In order to evaporate the
HFIP, samples were kept overnight in a laminar flow cabinet.
Possible residues were removed in a SpeedVac device (SVR
2-18 Christ) for 10 min. Dried tubes were stored at − 20 °C.
For each assay, an aliquot was thawed and diluted in DMSO at
a concentration of 5 mM. This solution was further diluted in
PBS and incubated at 4 °C for 24 h. Alternatively, incubation
at 37 °C was also performed for fibrils formation. After incu-
bation, the solution was centrifuged at 14000g for 10 min and
the supernatant collected [39, 40]. To characterize the prepa-
ration, AβOs were separated by a 12% nondenaturing glycine
polyacrylamide gel electrophoresis. Then, gel was stained
with a Coomassie G250 solution (0.08% Coomassie
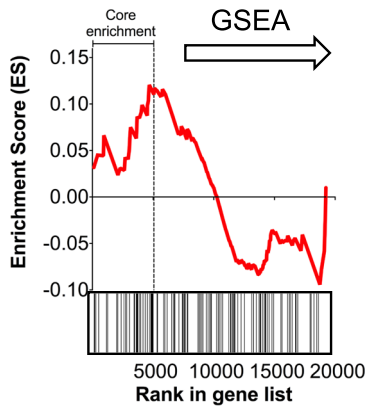(Sigma); 1.6% H_3PO_4; 8% $(NH_4)_2SO_4$; 20% methanol).

Cytotoxicity Parameters

Cytotoxicity induced either by OA (Sigma-Aldrich®) or
AβOs in RA + BDNF-differentiated cells was analyzed using
the 3-(4,5-dimethylthiazol-2-yl)-2,5-diphenyltetrazolium bro-
mide (MTT) (Sigma-Aldrich®) assay. For this assay, SH-
SY5Y cells were seeded in 24-well plates at density of 6×10^4 cells per well and treated with increasing amounts of OA
or AβOs in order to determine sublethal doses. After 24 h
treatment, cells were incubated with 0.5 mg/mL MTT for
1 h at 37 °C. DMSO was added to solubilize formazan crys-
tals. The absorbance was measured at 560 nm and 630 nm in a
plate reader (SoftMax Pro, Molecular Devices, USA).

Statistical Analysis

Band intensities of Western blots were quantified using
ImageJ and expressed as relative values to the controls. Data

Fig. 3 Effect of the differentiation protocol on gene expression. ▶
Differential expression of cholinergic synapse and Alzheimer's Disease
network genes mediated by treatment with RA + BDNF in human SH-
SY5Y neuroblastoma lineage. Here are shown genes belonging to the
gene interaction network of cholinergic synapse (**a**) and Alzheimer's
Disease network (**b**), from KEGG platform, and genes that showed sig-
nificant modulation in their expression by treatment with RA and BDNF
compared to treatment with RA. Genes were ranked based on the corre-
lation between their expression and the class distinction

a)

Cholinergic synapse network

GSEA

Core enrichment

Enrichment Score (ES): 0.15, 0.10, 0.05, 0.00, -0.05, -0.10
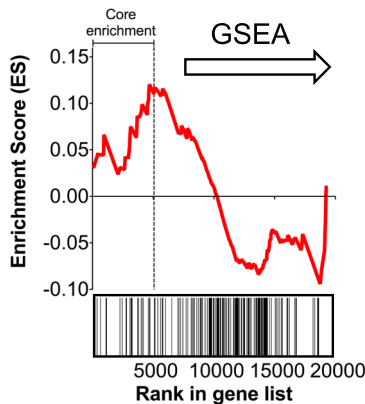
Rank in gene list: 5000 10000 15000 20000

*Data generated with gene set enrichment analysis (GSEA) comparing 7-day RA + BDNF-differentiated cells (n = 2) *vs.* 7-day RA-differentiated SH-SY5Y cells (n = 4) transcripts obtained as described in *"Materials and Methods"*.

Genes from Cholinergic synapse network enriched in RA + BDNF cells*

Heat map	Symbol	Gene name
	GNGT1	G Protein Sub. Gamma Transducin 1
	CACNA1F	Voltage-Gated Ca Channel Sub. Alpha1 F
	ADCY4	Adenylate Cyclase 4
	CHRNA6	Cholinergic Receptor Nicotinic Alpha 6
	ADCY8	Adenylate Cyclase 8
	CAMK2A	Ca/Calmodulin-Dependent Kinase II Alpha
	PRKCG	Protein Kinase C Gamma
	CACNA1A	Voltage-Gated Ca Channel Sub. Alpha1 A
	CACNA1D	Voltage-Gated Ca Channel Subunit Alpha1 D
	PIK3CG	Phosphatidylinositol-4,5-Bis-P 3-Kinase Gamma
	ADCY2	Adenylate Cyclase 2
	GNG13	G Protein Sub. Gamma 13
	CHRM4	Cholinergic Receptor Muscarinic 4
	CHRM3	Cholinergic Receptor Muscarinic 3
	ADCY5	Adenylate Cyclase 5
	KCNQ3	Voltage-Gated K Channel Subf. Q Member 3
	CHAT	Choline O-Acetyltransferase
	ITPR3	Inositol 1,4,5-Trisphosphate Receptor Type 3
	KCNJ6	Voltage-Gated K Channel Subf. J Member 6
	CACNA1C	Voltage-Gated Ca Channel Sub. Alpha1 C
	PIK3R2	Phosphoinositide-3-Kinase Regulatory Sub. 2
	ACHE	Acetylcholinesterase
	GNG11	G Protein Sub. Gamma 11
	CREB3L3	CREB Protein 3-Like Protein 3
	PIK3CA	Phosphatidylinositol-4,5-Bis-P 3-Kinase Alpha
	GNGT2	G Protein Sub. Gamma Transducin 2
	KCNQ2	Voltage-Gated K Channel Subf. Q Member 2
	CHRNA4	Cholinergic Receptor Nicotinic Alpha 4 Sub.
	GNG2	G Protein Sub. Gamma 2
	PLCB2	Phospholipase C Beta 2
	KCNJ4	Voltage-Gated K Channel Subf. J Member 4
	PIK3R5	Phosphoinositide-3-Kinase Regulatory Subunit 5

b)

Alzheimer network

GSEA

Core enrichment

Enrichment Score (ES): 0.15, 0.10, 0.05, 0.00, -0.05, -0.10

Rank in gene list: 5000 10000 15000 20000

*Data generated with gene set enrichment analysis (GSEA) comparing 7-day RA + BDNF-differentiated cells (n = 2) *vs.* 7-day RA-differentiated SH-SY5Y cells (n = 4) transcripts obtained as described in *"Materials and Methods"*.

Genes from Alzheimer network enriched in RA + BDNF cells*

Heat map	Symbol	Gene name
	GRIN2A	Glutamate Ionotropic Receptor NMDA Sub. 2A
	CACNA1F	Voltage-Gated Ca Channel Sub. Alpha1 F
	NDUFA4L2	NADH Dehydrogenase 1 Alpha 4-Like 2
	TNF	Tumor Necrosis Factor
	CALML6	Calmodulin-Like Protein 6
	CALML3	Calmodulin Like 3
	CALML5	Calmodulin-Like Protein 5
	CACNA1D	Voltage-Gated Ca Channel Sub. Alpha1 D
	LRP1	LDL Receptor Related Protein 1
	COX4I2	Cytochrome C Oxidase Sub. 4I2
	BACE2	Beta-Site APP-Cleaving Enzyme 2
	COX6A2	Cytochrome C Oxidase Subunit 6A2
	COX8C	Cytochrome C Oxidase Subunit 8C
	MAPT	Microtubule Associated Protein Tau
	LPL	Lipoprotein Lipase
	COX6B2	Cytochrome C Oxidase Sub. 6B2
	ITPR3	Inositol 1,4,5-Trisphosphate Receptor Type 3
	CACNA1C	Voltage-Gated Ca Channel Sub. Alpha1 C
	BAD	BCL2 Associated Agonist Of Cell Death
	CASP12	Caspase 12 Pseudogene 1
	IL1B	Interleukin 1 Beta
	GRIN2B	Glutamate Ionotropic Receptor NMDA Sub. 2B
	ADAM10	ADAM Metallopeptidase Domain 10

were expressed as means ± SD from at least three independent experiments. Data from enzymatic analysis were expressed as percentage of untreated cells (mean ± SD) from at least four independent experiments. Multiple comparisons were analyzed by one-way analysis of variance (ANOVA) followed by Tukey's test, unless otherwise indicated. Differences were considered significant at $p < 0.05$. Statistical analyses were performed using the GraphPad® (San Diego, CA, USA, version 5.0).

Results

RA + BDNF-Differentiation Protocol Increased Neurite Density

The RA + BDNF-differentiation protocol is outlined in Fig. 1. Previously, our research group described that treatment with RA in combination with the reduction of FBS to 1% induced cell growth inhibition and neuronal morphology in SH-SY5Y cells, along with the expression of dopaminergic markers [21]. Based on this protocol, we added BDNF in the fourth and seventh day of differentiation. Although TrkB receptors are absent in undifferentiated SH-SY5Y cells, this cell line becomes responsive to BDNF treatment by previous incubation with RA [24]. Therefore, we analyzed the effect of RA differentiation protocol for 4 days on the expression of genes related to neurotrophin signaling network (Fig. 2a). Dozens of genes were upregulated by 4-day RA treatment including, as expected, the TrkB receptor gene (*NTRK2*). This molecular reprogramming justifies the remarkable neuronal morphology observed in cells treated with the RA + BDNF-differentiation protocol (Fig. 2b, c). When compared to RA treatment, BDNF-treated cells exhibited longer and more branched neurites, forming a robust neuritic network. Thus, our data confirm TrkB activation through RA treatment which allowed BDNF to induce a morphological differentiation. In light of this, we assessed the neurite density using immunocytochemistry via βIII-tubulin immunolabeling. Results revealed a two-fold increase in neurite density in RA + BDNF-differentiated cells compared to RA alone treatment (Fig. 2d).

### Cholinergic Synapse Pathway Is Enriched in RA + BDNF-Differentiation Protocol

Severe synaptopathy and loss of cholinergic neurons are major hallmarks of AD. Therefore, an important feature for an in vitro model of AD is based on the generation of human cholinergic neurons that express AD-relevant genes. Our RA + BDNF-differentiation protocol triggered an enrichment of key elements from the cholinergic synapse and Alzheimer's networks (gene list curated by KEGG—pathways) (Fig. 3). This analysis showed an increased expression of choline *O*-

Fig. 4 Effects of RA + BDNF-differentiation on cholinergic markers. **a** AChE activity determined by the kinetics of formation of sulfhydryl groups (-SH) released from acetylthiocholine degradation during 10 min. Data presented as mean ± SD for four independent experiments performed in triplicates (ANOVA, *$p < .05$, **$p < .01$, ***$p < .001$). **b** ChAT activity determined by the kinetics of formation of CoA and 4-TP conjugate for 90 min. Data presented as mean ± SD for four independent experiments performed in duplicates. (ANOVA, ***$p < .001$). **c** Densitometry and representative image of Western Blot main marker of cholinergic neurons. Data presented as mean ± SD of three experiments. (ANOVA, *$p < .05$). **d** Densitometry and *Western blotting* of the dopaminergic neuron marker. Analysis of the bands represented by mean ± SD of three independent experiments. **e** RT-qPCR from undifferentiated, RA-treated or BDNF+RA-treated SH-SY5Y cells for 7 days. mRNAs were isolated, transcribed into cDNAs, and RT-qPCR was performed as described. Gene expression was quantified by $\Delta\Delta CT$ method and normalized using *RACK1* in three independent experiments. Multiple comparisons were analyzed by ANOVA followed by Mann-Whitney *U* test. Data was considered significant at *$p < .05$

acetyltransferase (*CHAT*), acetylcholinesterase (*ACHE*), cholinergic receptors (*CHRNA6*, *CHRM4*, *CHRM3* and *CHRNA4*) (Fig. 3a), and important key genes related to AD cascade such as the beta-site APP-cleaving enzyme 2 (*BACE2*), microtubule-associated protein Tau (*MAPT*), and ADAM metallopeptidase 10 (*ADAM10*) (Fig. 3b).

Cholinergic Markers Have Increased Expressions and Activities in RA + BDNF-Differentiated Cells

Effects of sequential RA + BDNF treatment on the enzymatic activities of cholinergic markers (such as AChE and ChAT) in each of the experimental groups were evaluated in order to characterize a potential cholinergic differentiation. AChE is the primary cholinesterase in the body and catalyzes the breakdown of acetylcholine (ACh) and other choline esters that function as neurotransmitters [3]. Even though RA treatment induced an increase in AChE activity in relation to nondifferentiated cells, the combination of RA with BDNF revealed a significant enhancement in AChE activity ($p < 0.05$) compared to other treatments (Fig. 4a). Similarly, ChAT activity ($p < 0.01$) (Fig. 4b) and protein levels ($p < 0.01$) (Fig. 4c) were significantly increased in RA + BDNF-treated cells. ChAT is a transferase responsible for the synthesis of ACh and its presence classifies the nerve cell as a cholinergic neuron [3, 41]. However, studies have shown that several other neuronal proteins have their expression increased by BDNF [25]. This raised the question whether BDNF, as a neurotrophic factor, caused an indiscriminate increase in neuronal markers. Therefore, we analyzed DAT expression by *Western blot*, a widely used dopaminergic marker [11] (Fig. 4d). Interestingly, DAT levels were increased only in RA-differentiated SH-SY5Y, as previously described by our group [22]. Moreover, qPCR analysis showed slightly increased cDNA levels of important AD genes in RA + BDNF-
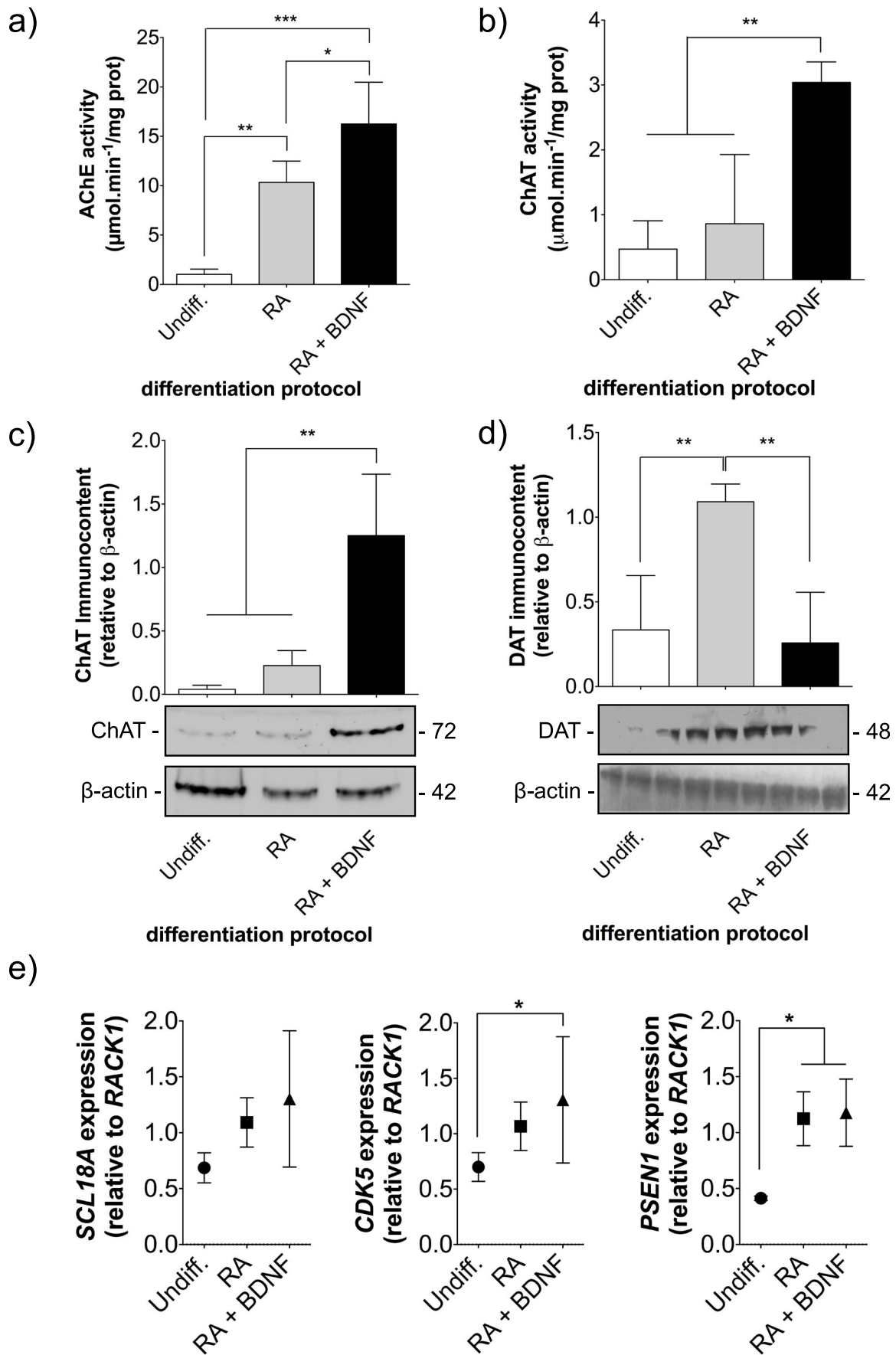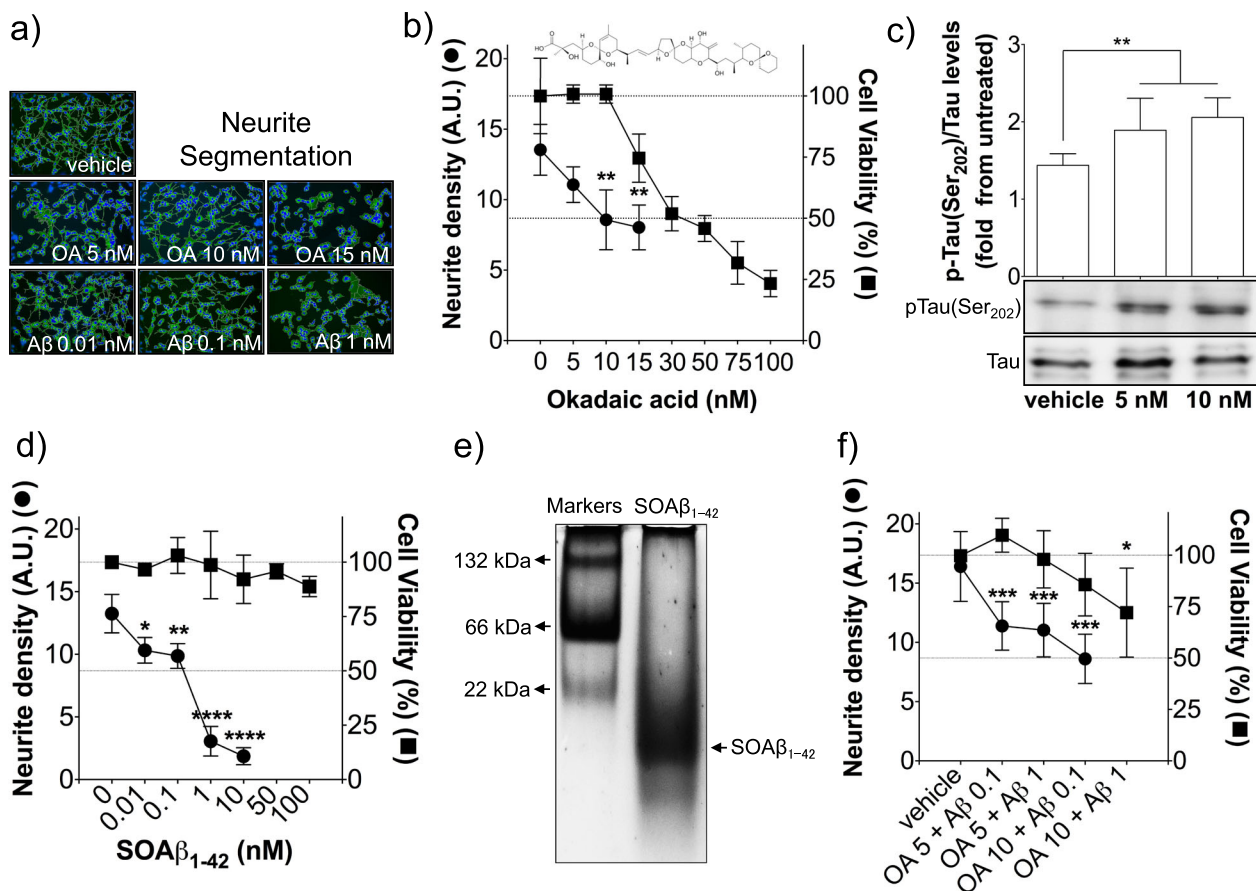
Fig. 5 Characterization of an AD-like in vitro model. **a** Representative images of RA + BDNF-differentiated cells treated with distinct doses of OA or soluble Aβ oligomers. Overlapping of βIII-tubulin and Hoechst 33342 and further segmentation performed by AutoQuant Neurites Software. **b** Graph displaying quantification of segmented images (left axis) showing the effects of OA toxicity on neurite density. Five randomly selected images were captured from each of three independent experiments A.U., arbitrary units. On the right axis, the cytotoxicity of the drug was assessed by the MTT assay. Data presented as mean ± SD for four independent experiments performed in triplicates. (ANOVA *p < .05). **c** Densitometry and representative Western blot of the hyperphosphorylated Tau immunocontent. Membranes were tested for p-Tau Ser202. Analysis of the bands represented by mean ± SD of two independent experiments. **d** Graph representing, on the left axis, the neurite density per cell body, showing the neurotoxic effect of treatment with Aβ. On the right axis, treatment with soluble βA oligomers effects on cell viability determined by the MTT assay. Data presented as mean ± SD for three independent experiments performed in triplicates. (ANOVA, *p < .05). **e** Representative gel electrophoresis of the preparation of soluble oligomers from Aβ$_{(1-42)}$. **f** Effect of the combination of sublethal doses of OA and Aβ oligomers. Graphs showing neurite density and cell viability. Data presented as mean ± SD for three independent experiments performed in duplicates

differentiated cells such as *SCL18A*, which encodes the vesicular acetylcholine transporter (vAChT) ($p < 0.05$), *CDK5* (cyclin-dependent kinase 5) which dysregulation has been implicated in AD ($p < 0.05$), and *PSEN1* (presenilin-1, a member of the gamma secretase complex, which has an important role in generation of Aβ from APP) ($p < 0.05$) (Fig. 4e). These data suggest that our differentiation protocol induces a predominantly cholinergic phenotype in SH-SY5Y with increased expression of AD-relevant proteins.

Characterization of an AD-Like In vitro Model

The RA + BDNF-differentiated cells were then used for mimicking pathological events typically found in early stages of AD. To do so, we challenged our cells with OA and AβOs and

evaluated neuronal cell viability (by MTT assay) and neurite densities as measurements of neurotoxic endpoints. OA is a serine/threonine phosphatase 1 (PP1) and 2A (PP2A) inhibitor that can lead to increased phosphorylated/dephosphorylated tau ratio, since dephosphorylation of this protein is mainly mediated by these phosphatases [42]. Neurites in RA + BDNF-differentiated SH-SY5Y cells were highly sensitive to OA treatment in the low nanomolar range (10–15 nM) ($p < 0.01$) (Fig. 5b). Moreover, treatment with 5 nM and 10 nM OA in RA + BDNF-differentiated cells, which was demonstrated to be in the sublethal range of the drug ($EC_{50} = 36$ nM) (Fig. 5b), was able to demonstrate tau hyperphosphorylated at Ser202 ($p < 0.01$) (Fig. 5c).

Subsequently, we studied the neurotoxic effect of AβOs on RA + BDNF-differentiated SH-SY5Y cells. AβOs were

highly synaptotoxic in RA + BDNF-differentiated SH-SY5Y cells, as measured by neurite density, even at concentrations as low as 0.01 nM ($p < 0.05$) (Fig. 5d). It is possible that the dehydrogenases that metabolize MTT to formazan salt were still active in the soma of neurons whereas AβOs toxic effects induced the retraction of neurites.

We then chose sublethal doses of each neurotoxin to characterize a cell model mimicking early stages of AD. As shown in Fig. 5f, SH-SY5Y cells were treated with a combination of selected OA and AβOs concentrations. We observed that, whereas the combination of 10 nM OA with 0.1 nM AβOs induced a low death rate, neuritic density was drastic reduced ($p < .0001$).

Discussion

This study reveals a significant increase in neurite density when BDNF was added to the RA-differentiation protocol, indicating a switch to a neuronal phenotype resembling a highly connected synaptic network. Moreover, we observed higher expression and enzymatic activities of cholinergic markers in RA + BDNF-treated cells. These findings suggest that this differentiation protocol induces a shift to a neuronal phenotype with predominantly cholinergic features. Next, differentiated cells were exposed to sublethal doses of OA and AβOs (Fig. 5a–f) which might recapitulate early stages of tau and amyloid pathology, respectively. The combination of sublethal doses of OA and AβOs in the treatment of differentiated SH-SY5Y cells provides an in vitro model resembling the pathophysiology of cholinergic neurons initially affected by AD. In general, detection of AD symptoms occurs in a very advanced stage of disease where the inhibition or reversal of the disease progression is a great challenge [43]. In addition, as few AD models have clear cholinergic loss, the establishment of a cholinergic differentiation protocol for SH-SY5Y cells seems an important step for characterizing a suitable AD in vitro model.

TrkB receptors are expressed under the RA-inducing activity, switching on the TrkB-centered signaling pathways which eventually affects cell survival, axonal outgrowth, and cell differentiation. Thus, the RA-differentiation effect upon SH-SY5Y cells can be potentiated by the addition of BDNF [24]. The addition of BDNF on the fourth day of RA-treated cells produced morphological alterations indicating that RA was able to induce the expression of TrkB receptors early in treated neuroblastoma SH-SY5Y cells [25]. The heat map diagram of differential gene expression (Fig. 2a) showed enrichment of NTRK2 gene. Moreover, the expression of a number of downstream genes of the TrkB signaling cascade was also enhanced, such as SHC, AKT, and genes encoding subunits of PI3K.

At the gene expression level, cholinergic synapse and AD networks are enriched following addition of BDNF to RA-treated cells. Biochemical analysis also showed higher cholinergic protein expression and activity under same treatment conditions. Cholinergic neurons are especially vulnerable in AD playing a significant role in cognitive impairment [4, 41, 44]. Therefore, studies focusing on cholinergic markers provide insight into the pathophysiological conditions of the disease. Indeed, anticholinesterase inhibitors are currently approved for treating AD and are temporarily effective for attenuating cognitive symptoms [45]. Both microarray and RT-PCR analysis demonstrated that the RA + BDNF-differentiation protocol promoted the expression of CHAT, ACHE, and important cholinergic receptors (Fig. 2). The expression of SLC18A3 gene, which encodes the transmembrane protein vAChT, is also increased. vAChT is responsible for the transportation of ACh into secretory vesicles to be released into the extracellular space [46]. Interestingly, AD network was found enriched in RA + BDNF-treated cells. Important genes related to AD pathophysiology such as PSEN1, BACE2, MAPT, and ADAM10 were found to have its expression enriched. BACE2 gene, a BACE1 homolog, is also responsible for the proteolytic processing of the APP and it is associated to AD pathology [47, 48]. PSEN1 encodes the protein presenilin-1, which is a subunit of the gamma-(γ)-secretase complex responsible for the cleavage of a variety of transmembrane proteins. Mutations in the PSEN1 gene are the most common cause of early-onset AD, accounting for up to 70% of cases [49]. A disintegrin and metalloproteinase domain-containing protein 10 is the protein encoded by the ADAM10 gene that cleaves several membrane proteins at the cellular surface, including APP. This is the main α-secretase in the brain and it accounts for the releasing of neuroprotective soluble APPα fragments [50]. Further, results from RT-PCR have shown enhanced expression of CDK5 gene. CDK5 is involved in cell survival pathways and its deregulation contributes to the development of AD neurodegenerative features. This proline-directed serine/threonine protein kinase is implicated in mitochondrial dysfunction and induction of Aβ production and accumulation [51]. Taken together, our differentiation protocol induces the expression of cholinergic markers and genes already reported to be associated with AD. With this in mind, this cell model enables the investigation of mechanisms linked to AD pathophysiology.

Neuronal information processing is highly dependent upon synaptic connectivity. Therefore, neuronal arborization is a crucial morphological parameter for determining neuronal survival [52]. When cells were treated with OA, we observed that the reduction in neurite density and cell viability occurred in a dose-dependent manner. In addition, an increase in phosphorylated tau at Ser_{202} (Fig. 5c). OA inhibits the action of phosphatases 1 and 2A responsible for the dephosphorylation of tau protein. Abnormal phosphorylation might initially occur at Ser_{202} site in dystrophic neurites [53]. This also corroborates with data in the literature indicating that hyperphosphorylation

of Tau and its subsequent deposition are related to the degeneration of neurons in brains of AD patients [6].

Regarding the role played by Aβ in AD, recent studies suggest that AβOs can alter neurotransmitter release such as ACh [54]. Interestingly, low doses of OA and AβOs induced a severe decrease in neurite density but only a slight decrease in cell viability (Fig. 5d). Many neurotoxic insults can cause neurite retraction. Studies indicate that altered retraction and elongation might disturb neurite outgrowth homeostasis and induce tau pathology [55, 56], which correlates with neurodegeneration [57]. Aβ oligomers have been identified in different stages of AD, and studies suggest that they could be used as biomarkers in the early preclinical stages of the disease [58]. Here, we described the characterization of an AD-like in vitro model using SH-SY5Y cells and challenged this cell line with AβOs and okadaic acid. Low doses of neurotoxins used in the treatment of SH-SY5Y cells were chosen with the purpose of subsequently selecting one that does not compromise drastically the basic functionality of the cells, in order to study mechanisms that lead to early synaptic dysfunction.

Age-related neurodegenerative diseases such as Alzheimer's are largely human-specific diseases and represent the interface of environmental factors, genetics, epigenetics, and the aging process per se [2, 5]. Even though most of the current models only take into account one of these factors and therefore do not reproduce the complexity of the diseases, cell models, such as the described here, provide a simple, inexpensive, and potentially useful tool for the dissection of the basic disease mechanisms and the screening of compounds targeting specific mechanisms involved in AD.

Conclusion

Few AD models reproduce the cholinergic loss found in the disease [45]. In this work, human neuroblastoma SH-SY5Y cells were differentiated into a neuronal phenotype with cholinergic features. While it is not clear yet how AD early signs are developed, it is known that pathophysiological abnormalities precede clear clinical symptoms [43]. By challenging these cells, we attempted to mimic initial stages of neuronal death by Aβ and tau pathology. Our preliminary results highlighted the potential applicability of this cell model as a useful tool for AD research. The in vitro model proposed here might be convenient for performing fast high-throughput neuroprotective drugs screening for reversing or inhibiting damage caused by neurotoxins involved in AD pathology.

References

1. Moller HJ, Graeber MB (1998) The case described by Alois Alzheimer in 1911. Historical and conceptual perspectives based on the clinical record and neurohistological sections. Eur Arch Psychiatry Clin Neurosci 248:111–122
2. Forman MS, Trojanowski JQ, Lee VM (2004) Neurodegenerative diseases: a decade of discoveries paves the way for therapeutic breakthroughs. Nat Med 10:1055–1063
3. Oda Y, Nakanishi I (2000) The distribution of cholinergic neurons in the human central nervous system. Histol Histopathol 15:825–834
4. Nyakas C, Granic I, Halmy LG, Banerjee P, Luiten PGM (2011) The basal forebrain cholinergic system in aging and dementia. Rescuing cholinergic neurons from neurotoxic amyloid-β42 with memantine. Behav Brain Res 221:594–603
5. Reitz C, Mayeux R (2014) Alzheimer disease: epidemiology, diagnostic criteria, risk factors and biomarkers. Biochem Pharmacol 88: 640–651
6. Adalbert R, Gilley J, Coleman MP (2007) Aβ, tau and ApoE4 in Alzheimer's disease: the axonal connection. Trends Mol Med 13: 135–142
7. Pagani L, Eckert A (2011) Amyloid-β interaction with mitochondria. Int J Alzheimers Dis 2011:925050
8. Deshpande A, Mina E, Glabe C, Busciglio J (2006) Different conformations of amyloid beta induce neurotoxicity by distinct mechanisms in human cortical neurons. J Neurosci 26:6011–6018
9. Gouras GK, Tampellini D, Takahashi RH, Capetillo-Zarate E (2010) Intraneuronal amyloid-β accumulation and synapse pathology in Alzheimer's disease. Acta Neuropathol 119:523–541
10. Wang H-W, Pasternak JF, Kuo H, Ristic H, Lambert MP, Chromy B et al (2002) Soluble oligomers of beta amyloid (1-42) inhibit long-term potentiation but not long-term depression in rat dentate gyrus. Brain Res 924:133–140
11. Agholme L, Lindström T, Kågedal K, Marcusson J, Hallbeck M, Kgedal K et al (2010) An in vitro model for neuroscience: differentiation of SH-SY5Y cells into cells with morphological and biochemical characteristics of mature neurons. J Alzheimers Dis 20: 1069–1082
12. Carolindah MN, Rosli R, Adam A, Nordin N (2013) An overview of in vitro research models for Alzheimer's disease. Regen Res 2:8–13
13. Gu H, Li L, Cui C, Zhao Z, Song G (2017) Overexpression of let-7a increases neurotoxicity in a PC12 cell model of Alzheimer's disease via regulating autophagy. Exp Ther Med 14:3688–3698
14. Kovalevich J, Langford D (2013) Considerations for the use of SH-SY5Y neuroblastoma cells in neurobiology. Methods Mol Biol 1078:9–21
15. Choi SH, Kim YH, Hebisch M, Sliwinski C, Lee S, D'Avanzo C et al (2014) A three-dimensional human neural cell culture model of Alzheimer's disease. Nature.
16. Biedler JL, Roffler-tarlov S, Schachner M, Freedman LS (1978) Multiple neurotransmitter synthesis by human neuroblastoma cell lines and clones. Cancer Res:3751–3757
17. Påhlman S, Ruusala a I, Abrahamsson L, Mattsson ME, Esscher T (1984) Retinoic acid-induced differentiation of cultured human neuroblastoma cells: a comparison with phorbolester-induced differentiation. Cell Differ 14:135–144
18. Påhlman S, Hoehner JC, Nånberg E, Hedborg F, Fagerström S, Gestblom C et al (1995) Differentiation and survival influences of growth factors in human neuroblastoma. Eur J Cancer 31A:453–458
19. Arcangeli A, Rosati B, Crociani O, Cherubini A, Fontana L, Passani B et al (1999) Modulation of HERG current and herg gene expression during retinoic acid treatment of human neuroblastoma cells: potentiating effects of BDNF. J Neurobiol 40:214–225
20. Encinas M, Iglesias M, Liu Y, Wang H, Muhaisen A, Cen V et al (2000) Sequential treatment of SH-SY5Y cells with retinoic acid

and brain-derived neurotrophic factor gives rise to fully differentiated, neurotrophic factor-dependent. J Neurochem 75:991–1003

21. Lopes FM, Schröder R, da Frota MLC, Zanotto-Filho A, Müller CB, Pires AS et al (2010) Comparison between proliferative and neuron-like SH-SY5Y cells as an in vitro model for Parkinson disease studies. Brain Res 1337:85–94

22. Constantinescu R, Constantinescu AT, Reichmann H, Janetzky B (2007) Neuronal differentiation and long-term culture of the human neuroblastoma line SH-SY5Y. J Neural Transm:17–28

23. Lopes FM, Londero GF, de Medeiros LM, da Motta LL, Behr GA, de Oliveira VA et al (2012) Evaluation of the neurotoxic/neuroprotective role of organoselenides using differentiated human neuroblastoma SH-SY5Y cell line challenged with 6-hydroxydopamine. Neurotox Res 22:138–149

24. Kaplan DR, Matsumoto K, Lucarelli E, Thiele CJ (1993) Induction of TrkB by retinoic acid mediates biologic responsiveness to BDNF and differentiation of human neuroblastoma cells. Neuron Neuron, **Cell Press** 11:321–331

25. Edsjö A, Lavenius E, Nilsson H, Hoehner JC, Simonsson P, Culp LA et al (2003) Expression of trkB in human neuroblastoma in relation to MYCN expression and retinoic acid treatment. Lab Investig 83:813–823

26. Ward NL, Hagg T (2000) BDNF is needed for postnatal maturation of basal forebrain and neostriatum cholinergic neurons in vivo. Exp Neurol 162:297–310

27. Schliebs R, Arendt T (2011) The cholinergic system in aging and neuronal degeneration. Behav Brain Res 221:555–563

28. Paul S, Jeon WK, Bizon JL, Han J-S (2015) Interaction of basal forebrain cholinergic neurons with the glucocorticoid system in stress regulation and cognitive impairment. Front Aging Neurosci 7:1–11

29. Ozen Irmak S, de Lecea L (2014) Basal forebrain cholinergic modulation of sleep transitions. Sleep 37:1941–1951

30. Haam J, Yakel JL (2017) Cholinergic modulation of the hippocampal region and memory function. J Neurochem 142:111–121

31. Grothe MJ, Schuster C, Bauer F, Heinsen H, Prudlo J, Teipel SJ (2014) Atrophy of the cholinergic basal forebrain in dementia with Lewy bodies and Alzheimer's disease dementia. J Neurol:71–73

32. Nilbratt M, Porras O, Marutle A, Hovatta O, Nordberg A (2010) Neurotrophic factors promote cholinergic differentiation in human embryonic stem cell-derived neurons. J Cell Mol Med 14:1476–1484

33. Sharow KA, Temkin B, Asson-Batres MA (2012) Retinoic acid stability in stem cell cultures. Int J Dev Biol 56:273–278

34. Gautier L, Cope L, Bolstad BM, Irizarry RA (2004) affy—analysis of Affymetrix GeneChip data at the probe level. Bioinformatics 20:307–315

35. Leek JT, Johnson WE, Parker HS, Jaffe AE, Storey JD (2012) The sva package for removing batch effects and other unwanted variation in high-throughput experiments. Bioinformatics 28:882–883

36. Subramanian A, Tamayo P, Mootha VK, Mukherjee S, Ebert BL (2005) Gene set enrichment analysis: a knowledge-based approach for interpreting genome-wide. PNAS 102:15545–15550

37. Ellman GL, Courtney KD, Andres V, Featherstone RM (1961) A new and rapid colorimetric determination of acetylcholinesterase activity. Biochem Pharmacol 7:88–95

38. Chao L, Wolfram F (1972) Spectrophotometric for choline acetyltransferase. Anal Biochem 46:114–118

39. Klein WL (2002) Aβ toxicity in Alzheimer's disease: globular oligomers (ADDLs) as new vaccine and drug targets. Neurochem Int 41:345–352

40. Stine WB, Dahlgren KN, G a K, LaDu MJ (2003) In vitro characterization of conditions for amyloid-beta peptide oligomerization and fibrillogenesis. J Biol Chem 278:11612–11622

41. Oda Y (1999) Choline acetyltransferase: the structure, distribution and pathologic changes in the central nervous system. Pathol Int 49:921–937

42. Kamat PK, Tota S, Saxena G, Shukla R, Nath C (2010) Okadaic acid (ICV) induced memory impairment in rats: a suitable experimental model to test anti-dementia activity. Brain Res 1309:66–74

43. Jack CR, Holtzman DM (2013) Biomarker modeling of Alzheimer's disease. Neuron 80:1347–1358

44. Schliebs R, Arendt T (2006) The significance of the cholinergic system in the brain during aging and in Alzheimer's disease. J Neural Transm 113:1625–1644

45. Douchamps V, Mathis C (2017) A second wind for the cholinergic system in Alzheimer's therapy. Behav Pharmacol 28:112–123

46. Butcher LL, Oh JD, Woolf NJ (1993) Cholinergic neurons identified by in sity hybridization histochemistry. In: Cholinergic Function and Dysfunction, AC Cuello, Ed., pp.1–8, Elsevier, Amsterdam, 1993

47. Mok KY, Jones EL, Hanney M, Harold D, Sims R, Williams J et al (2014) Polymorphisms in BACE2 may affect the age of onset Alzheimer's dementia in down syndrome. Neurobiol Aging 35:1513.e1–1513.e5

48. Ma Z, Jiang W, Zhang EE (2016) Orexin signaling regulates both the hippocampal clock and the circadian oscillation of Alzheimer's disease-risk genes. Sci Rep 6:36035

49. Kelleher RJ, Shen J (2017) Presenilin-1 mutations and Alzheimer's disease. Proc Natl Acad Sci 114:629–631

50. Endres K, Deller T (2017) Regulation of alpha-secretase ADAM10 in vitro and in vivo: genetic, epigenetic, and protein-based mechanisms. Front Mol Neurosci 10:1–18

51. Liu SL, Wang C, Jiang T, Tan L, Xing A, Yu JT (2016) The role of Cdk5 in Alzheimer's disease. Mol Neurobiol 53:4328–4342

52. van Pelt J, van Ooyen A, Uylings HBM (2014) Axonal and dendritic density field estimation from incomplete single-slice neuronal reconstructions. Front Neuroanat 8:1–16

53. Su JH, Cummings BJ, Cotman CW (1994) Early phosphorylation of tau in Alzheimer's disease occurs at Ser-202 and is preferentially located within neurites. Neuroreport 5:2358–2362

54. Olivero G, Grilli M, Chen J, Preda S, Mura E, Govoni S et al (2014) Effects of soluble β-amyloid on the release of neurotransmitters from rat brain synaptosomes. Front Aging Neurosci 6:166

55. Franze K, Gerdelmann J, Weick M, Betz T, Pawlizak S, Lakadamyali M et al (2009) Neurite branch retraction is caused by a threshold-dependent mechanical impact. Biophys J 97:1883–1890

56. Klein WL (2013) Synaptotoxic amyloid-beta oligomers: a molecular basis for the cause, diagnosis, and treatment of Alzheimer's disease? J Alzheimers Dis 33(Suppl 1):S49–S65

57. Lasagna-Reeves CA, Castillo-Carranza DL, Sengupta U, Sarmiento J, Troncoso J, Jackson GR et al (2012) Identification of oligomers at early stages of tau aggregation in Alzheimer's disease. FASEB J 26:1946–1959

58. Amaro M, Kubiak-Ossowska K, Birch DJS, Rolinski OJ (2013) Initial stages of beta-amyloid Aβ 1−40 and Aβ 1−42 oligomerization observed using fluorescence decay and molecular dynamics analyses of tyrosine. Methods Appl Fluoresc 1:15006